



# The Evolution of the $1/f$ Range Within a Single Fast-Solar-Wind Stream Between 17.4 and 45.7 Solar Radii

Nooshin Davis<sup>\*1</sup>, B. D. Chandran<sup>1</sup>, T. A. Bowen<sup>2</sup>, S. T. Badman<sup>3</sup>  
T. Dudok de Wit<sup>4,5</sup>, C. H. K. Chen<sup>6</sup>, S. D. Bale<sup>7,2</sup>, Zesen Huang<sup>8</sup>, Nikos Sioulas<sup>8</sup>, Marco Velli<sup>8</sup>

<sup>1</sup>University of New Hampshire <sup>2</sup>Space Science Lab, University of California, Berkeley <sup>3</sup>Harvard and Smithsonian <sup>4</sup>CNRS and University of Orleans  
<sup>5</sup>International Space Science Institute <sup>6</sup>Queen Mary University of London <sup>7</sup>University of California, Berkeley <sup>8</sup>University of California, Los Angeles  
<sup>\*</sup>Corresponding Author: Noshin.Mashayekhizadeh@unh.edu



## Introduction

Turbulence is a nonlinear phenomenon that allows transfer of energy between different scales.

The power spectrum of magnetic-field fluctuations in the fast solar wind ( $V_{SW} > 500 \text{ km s}^{-1}$ ) at magnetohydrodynamic (MHD) scales is characterized by two different power laws on either side of a break frequency  $f_b$ .

- The range  $f < f_b$ , is called the “energy-containing range”, and  $\alpha_B$  is often  $\approx -1$ , especially in the fast solar wind
- The range  $f > f_b$ , is called “inertial range”, and  $\alpha_B$  is approximately  $-5/3$  to  $-3/2$ .

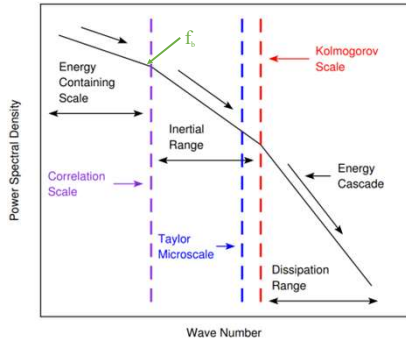


Figure 1: Generic picture of energy cascade in solar wind turbulence (Gurgiolo et al. 2013).

## Fast Solar Wind Stream

Data from Nov. 17-20, 2021 from PSP Encounter 10 is analyzed. The magnetic-field data used from the outboard flux magnetometer (MAG) (Bale et al., 2016) had a resolution of  $\sim 0.22 \text{ s}$ . The velocity data was derived from Solar Wind Electrons Alphas and Protons measurements (Kasper et al., 2016) at a resolution of  $\sim 3.49 \text{ s}$ .

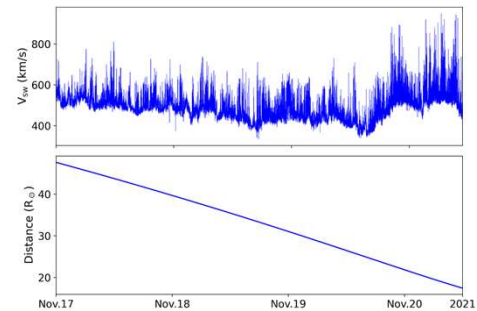


Figure 2: (top) Radial solar wind velocity (bottom) Heliocentric distance of PSP.

- Fast solar wind stream, with  $V_{SW} > 500 \text{ km/s}$  most of the time
- PSP orbit decreases from  $\sim 46$  to  $\sim 17 R_\odot$

## Parker Solar Probe Encounter 10

- Heliographic location varied by  $< 10^\circ$  in Carrington longitude.
- Field line mapping places the source region of solar wind near the center of the same coronal hole for the entire period.
- Time interval excludes both coronal mass ejection and any crossings of heliospheric current sheet.

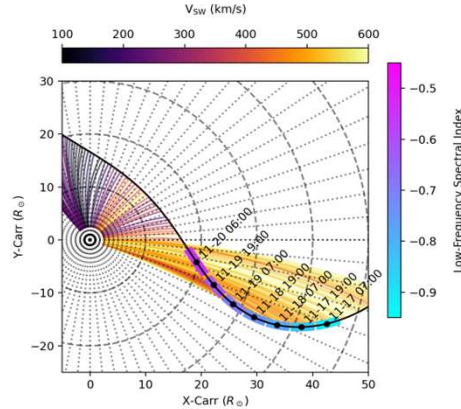


Figure 3: Orbit of PSP Encounter 10 and encountered solar wind.

**This time interval provides a nearly radial scan of the same fast solar wind stream from 17.4 to 45.7  $R_\odot$**

The angle  $\theta_{VB}$  between running one-hour averages of  $B$  and the spacecraft-frame velocity  $V$  is defined as:

$$\cos \theta_{VB} = \frac{\vec{V} \cdot \vec{B}}{|\vec{V}| |\vec{B}|}$$

- Most of the time  $160^\circ \lesssim \theta_{VB} \lesssim 180^\circ$ .
- $\sin(\theta_{VB})$  is small
- The frequency spectra at  $f < f_b$  corresponds approximately to the  $k_\parallel$  spectra of the low-frequency fluctuations.

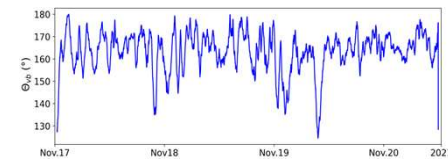


Figure 4: Variation of the angle between the mean magnetic field and mean velocity field in the spacecraft frame

**This fast solar wind stream's evolution towards a  $f^{-1}$  spectrum is similar to the nonlinear evolution of the PDI that takes place when slow waves are significantly dampened.**

## In Situ Development of the $f^{-1}$ Spectrum

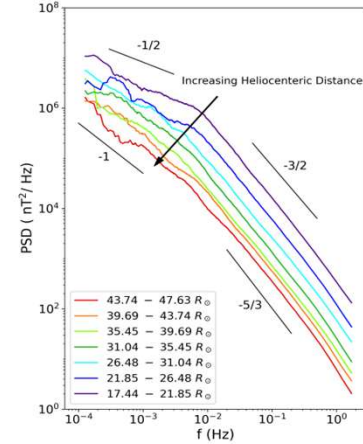


Figure 5: Magnetic field power spectrum for different heliocentric distances, with several power-law slopes marked for reference.

- As heliocentric distance increases, power levels decrease
- Total power decrease exceeds an order of magnitude over the range of distances considered
- This behavior is due to the expansion of the solar wind and the turbulent cascade.

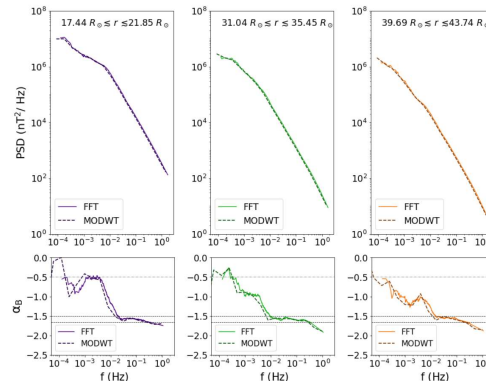


Figure 6: (top) Magnetic field power spectra (bottom) Local spectral index with horizontal lines for  $\alpha_B = -1/2, -3/2, \text{ and } -5/3$ .

**The power spectrum in the low frequency, inertial range gradually steepens towards a  $f^{-1}$  in situ as heliocentric distance increases**

## Radial Evolution of Spectral Index

- As heliocentric distance  $r$  increases from 17.4 to 45.7  $R_\odot$ , the spectrum steepens,  $\alpha_B$  decreases from  $-0.61$  to  $-0.94$
- The breakpoint frequency  $f_b$  decreases as  $r$  increases

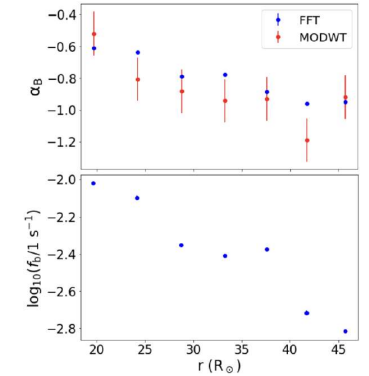


Figure 7: (Top) Variation of  $\alpha_B$ , and (Bottom)  $f_b$  with  $r$ .

- Possible physical mechanisms: (1) nonlinear interactions in reflection-driven Alfvén-wave turbulence or (2) nonlinear interaction evolution of the parametric decay instability

## Summary and Future Work

Key Points:

- $\alpha_B$  decreases from about  $-0.61$  to  $-0.94$  at  $f < 10^{-3} \text{ Hz}$  as  $r$  increases from 17.4 to 45.7  $R_s$ .
- Observations suggest that  $1/f$  is not produced at sun, but develops in situ, at least within fast wind.

Future Work:

- Revisit this behavior with further analysis of more solar-wind streams
- Investigate the physical mechanism(s) behind this behavior

## Acknowledgments

The authors are thankful to Aaron Roberts and the members of the FIELDS/SWEAP teams and PSP community for their helpful discussions.

## References

- [1] Badman, S. T., Riley, P., Jones, S. I., et al. 2023, Journal of Geophysical Research: Space Physics, 128, e2023JA031359
- [2] Bale, S. D., Goetz, K., Harvey, P. R., et al. 2016, SSRv, 204, 49
- [3] Chandran, B. D. G. 2018, JPIPh, 84, 905840106
- [4] Chen, C., Bale, S., Bonnell, J., et al. 2020, The Astrophysical Journal Supplement Series, 246, 53
- [5] Gurgiolo, C., et al. 2013, Ann. Geophys., 31, 2063-2075
- [6] Kasper, J. C., Abiad, R., Austin, G., et al. 2016, SSRv, 204, 131
- [7] Perez, J. C., Bourouaine, S., Chen, C. H. K., & Raouafi, N. E. 2021, 650
- [8] Tu, C.-Y., & Marsch, E. 1995, SSRv, 73, 1
- [9] Velli, M., Grappin, R., & Mangeney, A. 1989, PhRvL, 63, 1807
- [10] Verdini, A., Grappin, R., Pinto, R., & Velli, M. 2012, 256 ApJL, 750, L33